J Exp Biol Advance Online Articles. First posted online on 16 January 2014 as doi:10.1242/jeb.092726
Access the most recent version at http://jeb.biologists.org/lookup/doi/10.1242/jeb.092726

METHODS & TECHNIQUES

Simultaneous high-resolution pH and spectrophotometric recordings of oxygen binding in blood microvolumes

Michael Oellermann, Hans-O. Pörtner, Felix C. Mark*

Alfred Wegener Institute for Polar and Marine Research, 27570 Bremerhaven, Germany

*Author for correspondence (e-mail: FMark@awi.de)

Key words: Diffusion chamber, oxygen equilibrium curve, hemocyanin, haemocyanin, haemoglobin, pH optode, octopus, amphipod, Antarctic fish

Words main text: 3890

SUMMARY

Oxygen equilibrium curves have been widely used to understand oxygen transport in numerous organisms. A major challenge has been to monitor oxygen binding characteristics and concomitant pH changes as they occur *in vivo*, in limited sample volumes. Here we report a technique allowing highly resolved and simultaneous monitoring of pH and blood pigment saturation in minute blood volumes. We equipped a gas diffusion chamber with a broad range fibre optic spectrophotometer and a micro-pH optode and recorded changes of pigment oxygenation along PO_2 and pH gradients to test the setup. Oxygen binding parameters derived from measurements in only 15 µl of haemolymph from the cephalopod *Octopus vulgaris* showed low instrumental error (0.93%) and good agreement with published data. Broad range spectra, each resolving 2048 data points, provided detailed insight into the complex absorbance characteristics of diverse blood types. After consideration of photobleaching and intrinsic fluorescence, pH optodes yielded accurate recordings and resolved a sigmoidal shift of 0.03 pH units in response to changing PO_2 from 0-21 kPa. Highly resolved continuous recordings along pH gradients conformed to stepwise measurements at low rates of pH changes. In this study we showed that a diffusion chamber upgraded with a broad range spectrophotometer and an optical pH sensor accurately characterizes oxygen binding with minimal sample consumption and manipulation. We conclude that the modified diffusion chamber is highly suitable for experimental biologists who demand high flexibility, detailed insight into oxygen binding as well as experimental and biological accuracy combined in a single set up.

INTRODUCTION

Since the first oxygen binding experiments by Paul Bert (1878) and Carl Gustav von Hüfner (1890) and the pioneering work by Bohr, Hasselbalch and Krogh (1904) dating back more than a century, oxygen binding experiments have served to understand human blood physiology and diseases (e.g. Chanutin and Curnish, 1967; Festa and Asakura, 1979) or the environmental adaptation of various organisms (e.g. Brix, 1983; Herbert et al., 2006; Meir et al., 2009; Scott, 2011) and even resolved crime (Olson et al., 2010). Ever since, researchers have developed and refined techniques to comprehend the complex physiology of oxygen transport, leading to a variety of currently employed methods (Supplementary Table S1).

Such analysis commonly involves the determination of oxygen affinity (P_{50}). Accurate determination of P_{50} requires to control or monitor extrinsic factors like temperature, carbon dioxide (CO_2) and particularly pH. Assessing the effects of pH and the variation of pH during transition from the oxygenated to the deoxygenated state, due to the oxygenation dependent release or uptake of protons by the pigment (Haldane effect), requires knowledge of pH at different levels of saturation for the analysis of oxygen equilibrium curves (OEC). Conventionally, experimenters control pH by added buffers (e.g. Tris, HEPES, Brix et al., 1994) or determine pH from sub-samples or separately conditioned samples (e.g. Seibel et al., 1999; Weber et al., 2008) and rarely directly in the original sample (Pörtner, 1990; Zielinski et al., 2001). While added buffers prevent pH changes and may help to address specific functional characteristics of the pigment (e.g. effects of inorganic ions, Mangum and Lykkeboe, 1979) they disturb the fine tuning of oxygen binding (Brix et al. 1994) and block pH changes relevant as part of the oxygen transport process that need to be included for a comprehensive picture of oxygen transport *in vivo*. A major challenge in monitoring pH has been the relatively large sample volume required to immerse a pH electrode and its reference electrode. Particularly, analysis in highly limited sample volumes or devices that employ thin blood films (e.g. Diffusion chamber, HemOscan, Pwee 50, Supplementary Table S1) suffer from this constraint.

Further, while many commercially available devices have been designed for human or mammalian blood analysis (e.g. CO-Oximeter, HEMOX-Analyser) only few provide the flexibility needed for the analysis of non-model organisms bloods, characterized by small sample volumes, unusual spectra, extreme *in vitro* temperatures or high pH sensitivity.

Here we report a major step forward in the respective methodology, allowing the simultaneous analyses of pH and pigment absorbance in microvolumes of blood. The challenges successfully met by our technique comprise

(1) The parallel measurement of oxygenation, paired with the simultaneous monitoring of pH depending on oxygenation level.

(2) The use of minimal sample volumes of 15 µl.

(3) High resolution recordings, facilitated by continuous recordings of broad-range spectra and pH.

We upgraded a gas diffusion chamber (Niesel and Thews, 1961; Sick and Gersonde, 1969, 1972; Bridges et al., 1984; Morris and Oliver, 1999; Weber et al., 2010), with an integrated fibre optic micro-pH optode and a miniature broad range fibre optic spectrophotometer. The experimental setup offers high flexibility to produce accurate oxygen equilibrium curves and pH recordings from only minute volumes of sample.

RESULTS AND DISCUSSION

Spectrophotometric measurements

Using the modified diffusion chamber, we successfully performed measurements on haemolymph from *Octopus vulgaris* and *Eulimnogammarus verrucosus* and whole blood of *Pachycara brachycephalum* at various oxygen and carbon dioxide partial pressures and temperatures. The integrated broad range spectrophotometer resolved 2048 data points per spectrum from 200 to 1100 nm and yielded characteristic absorbance spectra for haemolymph containing haemocyanin with an oxygenation dependent peak at 347 nm (*Octopus vulgaris*, Figure 1A) and multiple responsive peaks at 540, 575, 412 and 335 nm for oxygenated and at 553, 427 and 366 nm for deoxygenated haemoglobin bearing blood (*Pachycara brachycephalum*, Figure 1B). In addition, to the haemocyanin peak at 336 nm, haemolymph from *Eulimnogammarus verrucosus* showed absorbance features above 400 nm that explain its green coloration (Figure 1C). The detailed broad range spectra strongly facilitate and enhance the analysis of solutions with complex absorbance spectra. Studies that gather only snap shots of the spectrum by means of single wavelength filters (e.g. Morris et al., 1985; Rasmussen et al., 2009) limit their experimental set up to a particular pigment type and may miss further relevant features.

The modified diffusion chamber yielded reproducible and accurate results employing both conventional stepwise measurements along a PO_2 gradient (Figure 2) as well as measurements along a pH gradient (Figure 3), designed for pH sensitive pigments like cephalopod haemocyanins (Pörtner, 1990). Oxygen equilibrium curves of *Octopus vulgaris* haemolymph constructed from five replicated experiments with discrete oxygenation steps at constant carbon dioxide partial pressure (PCO_2; 1 kPa) showed low variability among OECs and the derived parameters (Figure 2, Table 1, Supplementary Figure S4) with a relative error of 0.93% for oxygen affinity P_{50} and of 2.74% for the Hill coefficient n_{50}. This low instrumental error and the good agreement of P_{50} and n_{50} with published data on *Octopus vulgaris* haemolymph recorded at the same temperature and pH (Table 1, Figure 4), underline the accuracy of the setup. The Bohr coefficient recorded at 15°C was higher than reported in Brix *et* al. (1989) but closely matched values reported for *Octopus vulgaris* by Houlihan et al. (1982) and Bridges (1994) *Octopus dofleini* (-1.7 (pH 7.0-8.3), Miller, 1985) or *Octopus macropus* (-1.99 (pH 7.3-7.5), Lykkeboe and Johansen, 1982) (Figure 4, Table 1). The difference in Bohr coefficients towards the study by Brix et al. (1989) relates to the pH ranges

used to determine the Bohr coefficient. In octopods, P_{50} increases linearly with pH and levels off at lower pH (~7.0, Figure 4, Miller, 1985) as oxygen binding becomes pH insensitive (see 13 kPa OEC, Figure 3). Brix et al. (1989) included pH values below 7.0 (6.85-7.40), which consequently led to reduced regression slopes and underestimated Bohr coefficients. Thus, agreement with studies using pH ranges above 7.0 confirms the accuracy of Bohr coefficients determined with the modified diffusion chamber.

Both pigment absorbance and haemolymph pH responded to changes of gas composition within 30 seconds (Figure 5). The recording of one oxygen equilibrium curve, including calibration at 100% and 0% oxygen saturation, lasted on average 3.5 hours (± 0.23) for measurements (n = 5) with eight discrete oxygenation steps and 5.2 hours (± 0.21) for measurements (n = 4) with eight discrete pH steps. While the maximum absorbance signal at 347 nm (haemocyanin oxygenation peak) drifted by -3.5% (± 0.6%, n = 5) per hour, minimal absorbance remained nearly constant (0.27% ± 0.21%, n = 5). The protein peak drifted less and varied more among experiments (2.3% ± 2.7%, n = 5, Figure 5B). Negative drift observed for the maximum oxygenation signal was reported previously and explained by autoxidation of the blood pigment (Wells and Weber, 1989). Consequently, each measurement needs to comprise calibration steps with pure oxygen at the beginning and end to determine and include the apparent and constant drift in the calculation of pigment oxygenation by readjusting maximum absorbance at each consecutive oxygenation step (Wells and Weber, 1989). The less pronounced positive drift of the protein peak (Figure 5B) indicates a low degree of sample drying and no apparent dilution by condensation or denaturation of the haemolymph sample.

Interestingly, the height of the protein peak neither remained stable but increased/decreased upon oxygenation/deoxygenation (Figure 5, Supplementary Figure S5). This unexpected response of the protein peak to oxygenation/deoxygenation of the pigment (Figure 5, Supplementary Figure S5) cannot be ascribed to irreversible protein denaturation as the protein absorbance increased again upon re-oxygenation (Figure 5). Consequently, oxygenation status may affect protein absorbance spectra and thus measurements of protein concentration in haemolymph or blood. Conformational changes depending on the degree of oxygenation may affect the absorbance features of the aromatic tryptophan, tyrosine and phenylalanine residues that account for the absorbance at 270-295 nm (Alexander and Ingram, 1980). Although the protein peak may not always vary with oxygen content (Bolton et al., 2009), it would be advisable to test a given blood type for such oxygenation dependency.

pH recordings in blood microvolumes

Simultaneous monitoring of pH, using a pH micro-optode in the same 15 µl sample, yielded stable recordings within the calibrated range between pH 6.5-8.2. In response to changing oxygen partial pressure (PO_2; 0-21 kPa), these recordings were sufficiently precise to resolve a sigmoidal shift by 0.03 pH units, running reverse directional to the OEC (Figure 2). This shift denotes oxygenation dependent, lowered affinity of the pigment for protons (Haldane effect) and agrees well with other studies (e.g. *Carcinus maenas* ΔpH = 0.02 (Truchot, 1976). A sigmoidal rather than linear change of pH (Lapennas et al., 1981) may corresponds to the linked sigmoidal trajectory of oxygen binding. The continuous recording of pH further revealed pronounced but reversible decreases of ~0.1 pH units upon initial oxygenation, which indicates a high affinity state for protons in fully deoxygenated haemocyanins (Figure 5).

P_{50} derived from OECs recorded along pH gradients matched those recorded along PO_2 gradients and together showed a linear interdependence of pH and P_{50} in the pH range between 7.1 – 7.7 (Figure 4). The OEC recorded by a continuous decrease of pH was highly resolved (~500 data points, Figure 6) and fully equilibrated at slow PCO_2 changes of 0.015 kPa min^{-1}, as confirmed by the close match with the stepwise OEC (Figure 3). This further underlines the validity of this alternative methodology, designed for pH sensitive pigments. Simultaneous pH recordings here allow to construct highly resolved, continuous OECs from which blood parameters may be directly derived without curve modelling (Figure 3). At faster rates (0.045 kPa min^{-1}) the OEC shifted left as saturation required longer to stabilise than pH (Figure 3). A shift of continuous OEC at higher rates of PCO_2 or PO_2 changes has been explained by diffusion related, dislike durations between sensor and sample to fully equilibrate with the surrounding gas (‘dynamic error’, Lapennas et al., 1981). However, as the pH optode was immersed in the sample, gas diffusion rates between sample and sensor were likely similar, suggesting some delay in oxygenation of octopus haemocyanin in response to pH changes.

The signal of the pH optode drifted by -0.016 pH units per 100 recordings (± 0.004) and was corrected accordingly (Figure 5A). This drift was higher than stated by the manufacturer (-0.0035 pH units per 100 recordings, Manufacturer manual, Presens, 2004, 2012), probably due to incomplete protection from the light beam of the UV-VIS light source and resulting photobleaching of the optode’s fluorescent dyes. Thus, pH optodes may be re-calibrated prior

to each measurement and the pH signal corrected for instrumental signal drift. Light exposure and therefore pH signal drift can be reduced by a software-controlled shutter in the light path that opens only during measurements or by using optically isolated sensor tips. The pH signal was also corrected for autofluorescence emitted by the sample, which decreased the pH signal in haemolymph by 0.06 units. Optical isolation but also calibration in the analysed medium can reduce or prevent the effects by intrinsic fluorescence between 530 – 660 nm, caused by e.g. porphyrine structures, which affect phase and amplitude of the pH raw signal (PreSens, personal communication, Sept 10, 2013).

Advantages and disadvantages

The modified diffusion chamber benefits the analysis of oxygen binding in several ways. Simultaneous recording of pigment oxygenation and pH allows to characterise oxygen binding and intrinsic pH responses under close to *in vivo* conditions. Minute sample volumes facilitate the analysis of blood from small organisms or less invasive and repeated sampling from the same individual. Small sample volumes reduce the need to pool blood, facilitate replicate measurements and shorten measurement time due to accelerated gas equilibration. Highly resolved broad-range spectra capture detailed spectral properties of the pigment and promote the analysis of diverse blood types. Thin optical microsensors (for pH or PO_2) deliver stable and rapid recordings down to 0°C (own observation) and allow to record continuous and highly resolved OECs (Figure 3). The gain of details improves the accuracy of biophysical oxygen binding models, particularly if OECs do not follow a simple sigmoidal shape (Wells and Weber, 1989). The additional flexibility to operate at a large range of experimental temperatures and gas compositions makes this device not only highly suitable for standard applications but particularly for the functional analysis of blood from non-model organism.

The use of optical microsensors and thin layers of blood also require specific care. The fluorescent dyes of the pH optodes are prone to photobleaching, which can be overcome by optical isolation or determination and correction for signal drift. Effects by intrinsic fluorescence of the sample are resolved by optical isolation, calibration in the same type of sample or by an initial cross validation of pH with a pH electrode. The non-linear dynamic range of pH optodes restricts accurate recordings to pH values between 5.5-8.5, which however, suffices in most of the blood-physiological experiments. Optical pH sensors that cover the extreme and even the full pH range may remove this limitation soon (Safavi and Bagheri, 2003). Further, the 150 µm sensor tip breaks easily and requires careful handling.

Like pH electrodes, pH optodes require calibration with buffers of similar ionic strength as the sample analysed and at the same experimental temperature (Manufacturer manual, Presens, 2004). Some blood types may clog on the sensor tip, which can be avoided by bathing the pH optode in a heparin solution (1000 units ml^{-1}). Lastly, thin layers of blood are at higher risk to desiccate (Reeves, 1980), particularly at higher temperatures. Measures include decreased gas flow or covering of the blood sample with a gas permeable Teflon membrane (Reeves, 1980; Lapennas and Lutz, 1982; Clark et al., 2008).

CONCLUSION

In this study we showed that a diffusion chamber upgraded with a broad range spectrophotometer and a fibre optical pH sensor allows for parallel measurement of pH and pigment saturation in microvolumes of blood samples. The set up yields reproducible and accurate results and offers high flexibility regarding the type of samples and experimental settings. The availability of optical PO_2 or PCO_2 probes and the rapid development of other optical sensor types (e.g. nitrogen oxide) suggest a broad array of future implementations that will help to address novel biological questions.

MATERIAL AND METHODS

Experimental set up and modifications

A gas diffusion chamber (Eschweiler Co., Kiel, Germany) designed and described in detail by (Niesel and Thews, 1961; Sick and Gersonde, 1969, 1972) has been used to determine OECs by recording absorbance of a thin layer of a haemoglobin or haemocyanin bearing solution during continuous or stepwise changes of PO_2 (Wells and Weber, 1989). The original principle, characterised by full pigment deoxygenation with nitrogen gas followed by the time dependent diffusion of oxygenated gas into the chamber (Niesel and Thews, 1961; Sick and Gersonde, 1969), was essentially abolished in subsequent studies that continuously perfused the chamber with defined gas mixtures (e.g. Bridges et al., 1984; Morris and Oliver, 1999; Weber et al., 2010). We adopted this amendment and further modified the diffusion chamber as follows. (1) A broad range (200 to 1100 nm) fibre optic spectrophotometer (USB2000+, Ocean Optics, USA) was connected via two fibre optic cables fitted to the central cylinder of the diffusion chamber to direct the light beam via collimating lenses from the deuterium halogen light source (DT-Mini-2-GS, Ocean Optics, USA) through the sample glass plate back to the 2048-element CCD-array detector of the spectrophotometer (Figure 7, Supplementary Table S2). (2) The plastic slide that holds the sample glass plate in the light tunnel was modified to fit a fibre optic micro-pH optode (NTH-HP5-L5-NS*25/0.8-OIW, PreSens, Germany), housed in a syringe and connected to a phase detection device (µPDD 3470, PreSens, Germany, Figure 7, Figure 8). The needle of the syringe was then inserted through a silicone ring to prevent the leakage of gas (Figure 8). In contrast to pH electrodes, pH optodes exhibit very small sensor tips (<150 µm) and determine pH from the intensity ratio between two pH sensitive fluorescent dyes (Presens, 2004).

The water reservoir of the diffusion chamber was filled with a 20% ethylene glycol solution (anti-freeze agent, AppliChem, Germany) and the temperature monitored and controlled by means of a supplied temperature sensor (PreSens, Germany) and a connected circulating thermostatted water bath (LAUDA Ecoline Staredition RE 104, Germany). A gas mixing pump (Wösthoff, Germany) supplied an adjustable mixture of nitrogen, oxygen and carbon dioxide gas, humidified by an integrated scrubber to prevent desiccation of the sample (Figure 8).

Prior to each experiment, we performed a six point calibration (pH 6.7, 7.0, 7.2, 7.4, 7.7, 8.1) of the pH optode, in MOPS-buffered (40 mmol L^{-1}, 3-(N-Morpholino)-propanesulfonic acid),

filtered artificial sea water (35 psu) at the corresponding experimental temperature. pH of buffers was checked with a pH glass electrode (InLab Routine Pt1100, Mettler Toledo, Germany) and a pH meter (pH 330i, WTW, Germany), calibrated with low ionic strength pH standards (AppliChem, Germany, DIN19266) and corrected to the Free Scale pH with Tris-buffered seawater standard (Dickson, CO2 QCLab, batch 4 2010, USA, Riebesell et al., 2010) equilibrated at the same temperature. Aliquots of 18 µl of haemolymph (octopus/amphipod) were thawed on ice, shortly spun down to collect content (5 sec at 1000 *g*) and 0.35 µl of 0.2 mmol L^{-1} NaOH (4.6 µmol L^{-1} final concentration) added to raise haemolymph pH above 8.0 to ensure full pigment oxygenation. To avoid haemolysis and the formation of methaemoglobin by freezing, we used freshly sampled whole blood from *Pachycara brachycephalum* and diluted the sample with one volume of blood plasma to improve light transmission during the measurement. The pH of haemolymph/whole blood was not stabilized with extrinsic buffers such as Tris or HEPES as they disturb the effects by ligands and temperature on pigment oxygenation (Brix et al., 1994). We then spread out 15 µl of haemolymph/whole blood on the glass plate without contacting the sealing ring. The pH optode needle was inserted through the sealing ring and the sensor tip moved into the edge of the droplet to reduce bleaching of the dye by the light beam passing through the centre of the glass plate (Figure 8). Both the glass plate holder and the fitted pH optode were then inserted and fixed in the diffusion chamber (Figure 7). The spectrophotometer required the recording of light and dark spectra without blood sample before each measurement and was set to 15 milliseconds integration time, 100 scans to average and 30 seconds measurement intervals. pH drift of the pH optode was evaluated by measuring the pH difference of a MOPS buffered sea water pH standard (pH = 7.2) at 15°C before and after each experiment. Effects by intrinsic fluorescence were assessed by comparing pH recordings of the pH optode and the pH electrode in octopus haemolymph at 15°C.

Using *Octopus vulgaris* haemolymph we tested the setup via two previously employed methodologies. OECs were obtained 1) by stepwise changes of discrete PO_2 (1, 2, 4, 9, 13, 17, 21 kPa) at constant PCO_2 (e.g. Wells and Weber, 1989) or 2) by stepwise as well as continuous decreases of pH by means of increasing CO_2 concentrations (0–20 kPa) and constant PO_2 (e.g. Pörtner, 1990). While stepwise measurements allow the sample to fully equilibrate at several successive but discrete PO_2 or pH steps (Lapennas et al., 1981; Pörtner, 1990), continuous measurements characterize a constant change and monitoring of PO_2 or pH (Wells and Weber, 1989). Each experiment involved the calibration with pure nitrogen as well as pure oxygen at the beginning and at the end to determine the drift of the maximum

absorbance signal. The exemplary analysis of whole blood of *Pachycara brachycephalum* was performed from 21-0 kPa PO_2 and pH 8.2-7.1 at 0°C and of thawed haemolymph of *Eulimnogammarus verrucosus* at a constant PO_2 of 21 kPa and pH 7.7-6.9 at 6°C.

Animals

One major incentive to advance this method was to enhance the investigation of non-model organisms, which often suffer from instrumental restrictions (e.g. sample volume, wavelength filters, temperature setting) by devices optimised for human or rodent blood. We thus chose three non-model organisms with diverse experimental demands to test the flexibility and accuracy of the modified diffusion chamber. The cephalopod *Octopus vulgaris* (Lamarck, 1798) lives between 11 and 18°C and evolved a closed circulatory system containing blue haemolymph with the extracellular, pH-sensitive respiratory pigment haemocyanin at high concentrations (54.3 ± 6.9 g L^{-1}, Wells and Smith, 1987; Brix et al., 1989), which evolved independently from arthropod haemocyanin (van Holde et al., 2001). Published data on *Octopus vulgaris* blood physiology allowed us to test the accuracy of the modified diffusion chamber. The Antarctic eelpout *Pachycara brachycephalum* (Pappenheim 1912) lives at freezing temperatures, yields only little blood and circulates intracellular haemoglobin at - for teleosts - low concentrations (37.4 g L^{-1}) in a closed system. The Baikal amphipod *Eulimnogammarus verrucosus* (Gerstfeld, 1858) lives at 5-6°C and yields small amounts of green coloured haemolymph that transports oxygen via extracellular haemocyanin (45.3 ± 7.9 g L^{-1}) in an open vascular system (Wirkner and Richter, 2013).

Octopus vulgaris specimens were hand-caught by snorkelling at Banuyls sur Mer, France at 16°C. Animals were anaesthetised in 3% EtOH (Ikeda et al., 2009), and after withdrawing haemolymph from the cephalic vein, were finally killed by a cut through the brain following sampling. *Pachycara brachycephalum* was caught on Polarstern cruise ANTXXV/4 near Maxwell Bay at King George Island, Antarctica in May 2009 using fish traps, transported to the Alfred Wegener Institute, Bremerhaven, Germany and kept in aerated tanks connected to a re-circulating aquaculture system at 0°C. The animal was anaesthetised with 0.3 g L^{-1} tricaine methano-sulphonate (MS222), blood withdrawn using a heparinised syringe and finally killed by a spinal cut (Animal research permit no. 522-27-11/02-00(93), Freie Hansestadt Bremen, Germany). *Eulimnogammarus verrucosus* (Gerstfeld, 1858) was collected in Bolshie Koty, Lake Baikal, Russia during summer 2012, transported to Irkutsk, Russia and kept in aerated 2.5 l tanks at 6°C. Haemolymph was withdrawn using a dorsally inserted capillary. All

haemolymph samples were centrifuged at 15.000 *g* for 15 min at 0°C to remove cell debris and stored at -20°C.

Data analysis

The processing, time-matching and analysis of data from both the spectrophotometer and the pH meter were performed using the "R" statistical language (R Core Team, 2013) (R script see supplementary material S3).

An integrated five parameter logistic model (Equation 1, R "drc" add-on package (Ritz and Streibig, 2005) was applied to fit sigmoidal curves to stepwise OECs.

$$f(x,(b,c,d,e,f) = c + \frac{(d-c)}{\left(1+exp\left\{b\left(log\left(\frac{x}{e}\right)\right)\right\}\right)^{f}} \qquad (1)$$

The parameters *c* and *d* denote the upper and lower asymptotes and *f* the asymmetry of the curve. The parameters *b* and *e* correspond to the slope and inflection point of a four parameter logistic model if the parameter *f* equals 1. Note that this equation represents an empirical curve fit that does not describe the functional properties of the haemocyanin sub-units according to mechanistic insight.

Oxygen affinity (P_{50}) was interpolated from fitted OECs at half saturation and cooperativity (Hill's coefficient, n_{50}) determined via Hill plots by regressing $\log_{10}(Y/(1-Y))$ versus $\log_{10}PO_2$ in the linear mid-range (~20-80% saturation), with Y denoting the fractional saturation. The Bohr coefficient was calculated from the regression slope ($\Delta\log_{10}P_{50}$ versus ΔpH) between pH 7.1-7.7. In pH/saturation diagrams, P_{50} denotes the $\log_{10}$ of the oxygen isobar and the pH of the isobar at half saturation (pH_{50}, Pörtner, 1990). Data were expressed as means ± 95% confidence intervals if not stated otherwise.

LIST OF SYMBOLS AND ABBREVIATIONS

OEC	Oxygen equilibrium curve
PO_2	Oxygen partial pressure
PCO_2	Carbon dioxide partial pressure
P_{50}	Oxygen affinity
n_{50}	Hill coefficient

ACKNOWLEDGEMENTS

We would like to thank Dr. Jan Strugnell (La Trobe University, Bundoora) for providing lab space and her extensive support, Michael Imsic and all other staff and technicians of the La Trobe University for their kind support during the initial tests of the modified diffusion chamber; Erich Dunker, Matthias Littmann and Dirk Wethje (scientific workshop, Alfred Wegener Institute, Bremerhaven) for the technical modifications and drawings of the diffusion chamber, Lena Jakob, for providing haemolymph samples from *Eulimnogammarus verrucosus*; Marian Y Hu for his help to catch *Octopus vulgaris*; the logistics department of the Alfred Wegener Institute and last of all my wife and young son for their enriching company. We further would like to thank the two anonymous reviewers for their many helpful remarks and suggestions on an earlier version of this manuscript. We dedicate this article to the memory of Steve Morris and want to express our special thanks to Maria Morris and Elizabeth Morgan (University of Bristol) who saved and donated the diffusion chamber to our department.

FUNDING

This study was supported by a Journal of Experimental Biology travelling fellowship, a PhD scholarship by the German Academic Exchange Service (DAAD, D/11/43882) to MO, the Deutsche Forschungsgemeinschaft (MA4271/1-2 to FCM) and the Alfred Wegener Institute for Polar and Marine Research.

AUTHOR CONTRIBUTIONS

MO and FCM developed the technical modifications, compiled the manuscript and interpreted results. MO performed the experiments and analysis. HOP initiated the discussion and contributed to data interpretation and manuscript editing.

FIGURE LEGENDS

Figure 1: (**A**) Broad range spectra of haemolymph from *Octopus vulgaris* (15°C), measured at 4 kPa PO_2 from high to low pH (ca. 8.2-6.8). Exemplary, broad range spectral recordings of whole blood from (**B**) the Antarctic eelpout *Pachycara brachycephalum* (0°C) and (**C**) of haemolymph from the Lake Baikal amphipod *Eulimnogammarus verrucosus* (6°C) reveal complex absorbance features. Spectral zones responding to oxygenation were marked by boxes and zoomed in. Spectra were coloured according to the visual appearance of the respective haemolymph/blood type. (Animal photos with permission by: Vladimír Motyčka, Christoph Held and Lena Jakob).

Figure 2: Replicated (n = 5) oxygen equilibrium curves of haemolymph from one *Octopus vulgaris* specimen obtained by stepwise changes to discrete PO_2 at constant PCO_2 (1 kPa). Five parameter logistic curves were fitted and individually plotted for each measurement to illustrate instrumental variability. Haemolymph pH (means ± S.E.M., blue), recorded by an optical pH microsensor immersed in the same sample droplet, changed sigmoidal and reverse directional to pigment saturation (black). The pH at half saturation (mean 7.23, ± S.E.M. 0.018) can be derived from the intersection between P_{50} (dashed line) and the fitted pH line.

Figure 3: Stepwise oxygen equilibrium curves (OEC) along a pH gradient (Pörtner, 1990), each derived from 15 µl haemolymph of *Octopus vulgaris* and measured by means of the modified diffusion chamber at 15°C and decreasing pH and various constant PO_2 (1, 4, 13, 21 kPa). The continuous OEC recorded at slow rates of PCO_2 changes (0.015 kPa min^{-1}, blue points) was highly resolved and closely matched the stepwise curves while at faster rates the OEC shifted left (dashed grey curve).

Figure 4: Bohr plot illustrating the pH dependence of oxygen affinity (P_{50}) of *Octopus vulgaris* haemolymph measured at 15°C. P_{50} from experiments with stepwise changes of PO_2 (filled circles) and pH (open circles) agreed with literature data (Brix *et* al. 1989, blue triangle and Bridges 1994, green square). The data point at 13 kPa was excluded from the linear regression fit as P_{50} leveled off at low pH (~7.0).

Figure 5: Response of **(A)** pH (uncorrected – grey trace, corrected by instrumental pH drift – blue trace) and **(B)** absorbance of the oxygenation dependent peak (347 nm) and the protein peak of *Octopus vulgaris* haemolymph to stepwise changes of PO_2 recorded at 15°C. Numbers above the absorbance trace indicate PO_2 of each oxygenation step. Horizontal

dashed lines indicate the change of maximal and minimum absorbance (at 347 nm) over time and vertical dashed lines the sudden but reversible pH changes upon initial oxygenation.

Figure 6: Number of data points (means ± 95% C.I.) for single oxygen equilibrium curves (OEC) compared between different methods (for references see supplementary table S7). The modified diffusion chamber method refers to continuous OEC measurements along a pH gradient.

Figure 7: (A) 3D model of the modified diffusion chamber and (B) a detailed cross section through the central cylinder of the gas diffusion chamber illustrating the embedded fibre optic micro-pH optode and an upper and lower custom made tube containing collimating lenses and fittings for in- and outgoing fibre optic cables of the light source and the broad range spectrophotometer. Illustrations were drawn with 3D CAD software (SolidWorks, version 12.0, files in supplementary material S6).

Figure 8: Detailed illustration of the pH optode housed in a syringe, mounted with a screw and fitted to a plastic holder, which is moved into the gas tight room centred in the diffusion chamber. The bended syringe needle is inserted through a silicon ring, which prevents gas leakage, and the sensor tip moved into the edge of the sample droplet located on a silica glass plate.

Table 1: Comparison of blood physiological parameters of *Octopus vulgaris* haemolymph with literature data. Bold values denote parameters recorded under the same conditions.

Table 1:

P_{50} (kPa)	n_{50}	Bohr coefficient	pH	Temp (°C)	Source
0.72	1.56		7.68		
1.72	1.59		7.45		
4.72 (0.07)	1.75 (0.07)	**-1.79** (pH 7.1-7.7)	7.23 (0.046)	15	This study
7.94	1.61		7.08		
2.20†	-		7.4		
2.45	1.5	**-1.34** (pH 6.85-7.4)	7.4	15	Brix *et* al. 1989
4.41	1.6	-1.10 (pH 6.85-7.4)	7.4	25	
3.20	2.6*		7.588		
4.09	2.9*	-1.58 / -1.73	7.520	22	Houlihan *et* al. 1982
4.80	3.5*	(pH 7.2-7.6 / 7.3-7.7)	7.415		
6.76	2.9*		7.327		
1.91	-	-1.86	7.4	10	Bridges 1994
2.61	-	**-1.83**	7.4	15	

*Hill coefficients were recalculated from Houlihan et al. 1982

†P_{50} extrapolated from linear regression line of Bohr plot at pH 7.4 (Figure 4)

REFERENCES

Alexander, J. B. and Ingram, G. A. (1980). A comparison of five of the methods commonly used to measure protein concentrations in fish sera. *J. Fish Biol.* **16**, 115-122.

Bert, P. (1878). La pression barométrique: recherches de physiologie expérimentale. Paris: G. Masson.

Bohr, C., Hasselbalch, K. and Krogh, A. (1904). Über einen in biologischer Beziehung wichtigen Einfluss, den die Kohlensäurespannung des Blutes auf dessen Sauerstoffbindung übt. *Skand. Arch. Physiol.* **16**, 402-412.

Bolton, J. C., Collins, S., Smith, R., Perkins, B., Bushway, R., Bayer, R. and Vetelino, J. (2009). Spectroscopic analysis of hemolymph from the American lobster (*Homarus americanus*). *J. Shellfish Res.* **28**, 905-912.

Bridges, C., Morris, S. and Grieshaber, M. (1984). Modulation of haemocyanin oxygen affinity in the intertidal prawn *Palaemon elegans* (Rathke). *Resp. Physiol.* **57**, 189-200.

Bridges, C. R. (1994). Bohr and root effects in cephalopod haemocyanins paradox or pressure in *Sepia officinalis*? *Mar. Freshw. Behav. Physiol.* **25**, 121-130.

Brix, O. (1983). Giant squids may die when exposed to warm water currents. *Nature* **303**, 422-423.

Brix, O., Colosimo, A. and Giardina, B. (1994). Temperature dependence of oxygen binding to cephalopod haemocyanins: ecological implications. *Mar. Freshw. Behav. Physiol.* **25**, 149-162.

Brix, O., Bårdgard, A., Cau, A., Colosimo, A., Condo, S. and Giardina, B. (1989). Oxygen-binding properties of cephalopod blood with special reference to environmental temperatures and ecological distribution. *J. Exp. Zool.* **252**, 34-42.

Chanutin, A. and Curnish, R. R. (1967). Effect of organic and inorganic phosphates on the oxygen equilibrium of human erythrocytes. *Arch. Biochem. Biophys.* **121**, 96-102.

Clark, T. D., Seymour, R. S., Wells, R. M. G. and Frappell, P. B. (2008). Thermal effects on the blood respiratory properties of southern bluefin tuna, *Thunnus maccoyii*. *Comp. Biochem. Physiol. Part A Mol. Integr. Physiol.* **150**, 239-246.

Festa, R. S. and Asakura, T. (1979). Oxygen dissociation curves in children with anemia and malignant disease. *Am. J. Hematol.* **7**, 233-244.

Herbert, Neill A., Skov, Peter V., Wells, Rufus M. G. and Steffensen, John F. (2006). Whole blood–oxygen binding properties of four cold temperate marine fishes: Blood affinity is independent of pH-dependent binding, routine swimming performance, and environmental hypoxia. *Physiol. Biochem. Zool.* **79**, 909-918.

Houlihan, D., Innes, A., Wells, M. and Wells, J. (1982). Oxygen consumption and blood gases of *Octopus vulgaris* in hypoxic conditions. *J. Comp. Physiol. B Biochem. Syst. Environ. Physiol.* **148**, 35-40.

Hüfner, G. (1890). Über das Gesetz der Dissociation des Oxyhaemoglobins und über einige daran sich knüpfende wichtige Fragen aus der Biologie. *Arch. Anat. Physiol.* **1**, 1-27.

Ikeda, Y., Sugimoto, C., Yonamine, H. and Oshima, Y. (2009). Method of ethanol anaesthesia and individual marking for oval squid (*Sepioteuthis lessoniana* Férussac, 1831 in Lesson 1830–1831). *Aquac. Res.* **41**, 157-160.

Lapennas, G. N. and Lutz, P. L. (1982). Oxygen affinity of sea turtle blood. *Resp. Physiol.* **48**, 59-74.

Lapennas, G. N., Colacino, J. M. and Bonaventura, J. (1981). Thin-layer methods for determination of oxygen binding curves of hemoglobin solutions and blood. In *Methods Enzymol.*, vol. Volume 76 (ed. L. R.-B. E. C. Eraldo Antonini), pp. 449-470: Academic Press.

Lykkeboe, G. and Johansen, K. (1982). A Cephalopod Approach to Rethinking about the Importance of the Bohr and Haldane Effects. *Pac. Sci.* **36**, 305-313.

Mangum, C. P. and Lykkeboe, G. (1979). The influence of inorganic ions and pH on oxygenation properties of the blood in the gastropod mollusc *Busycon canaliculatum*. *J. Exp. Zool.* **207**, 417-430.

Meir, J. U., Champagne, C. D., Costa, D. P., Williams, C. L. and Ponganis, P. J. (2009). Extreme hypoxemic tolerance and blood oxygen depletion in diving elephant seals. *Am. J. Physiol. Regul. Integr. Comp. Physiol.* **297**, R927-R939.

Miller, K. I. (1985). Oxygen equilibria of *Octopus dofleini* hemocyanin. *Biochemistry* **24**, 4582-4586.

Morris, S. and Oliver, S. (1999). Respiratory gas transport, haemocyanin function and acid-base balance in *Jasus edwardsii* during emersion and chilling: simulation studies of commercial shipping methods. *Comp. Biochem. Physiol. A* **122**, 309-321.

Morris, S., Taylor, A. C., Bridges, C. R. and Grieshaber, M. K. (1985). Respiratory properties of the haemolymph of the intertidal prawn *Palaemon elegans* (Rathke). *J. Exp. Zool.* **233**, 175-186.

Niesel, W. and Thews, G. (1961). Ein neues Verfahren zur schnellen und genauen Aufnahme der Sauerstoffbindungskurve des Blutes und konzentrierter Hämoproteidlösungen. *Pflügers Archiv* **273**, 380-395.

Olson, K. N., Hillyer, M. A., Kloss, J. S., Geiselhart, R. J. and Apple, F. S. (2010). Accident or arson: Is CO-Oximetry reliable for carboxyhemoglobin measurement postmortem? *Clin. Chem.* **56**, 515-519.

Pörtner, H. O. (1990). An analysis of the effects of pH on oxygen binding by squid (*Illex illecebrosus*, *Loligo pealei*) haemocyanin. *J. Exp. Biol.* **150**, 407.

Presens. (2004). Instruction manual pH-4 mini, pp. 51. Regensburg, Germany: Precision Sensing GmbH

Presens. (2012). Product sheet for pH microsensors, pp. 4. Regensburg, Germany: Precision Sensing GmbH

Rasmussen, J. R., Wells, R. M. G., Henty, K., Clark, T. D. and Brittain, T. (2009). Characterization of the hemoglobins of the Australian lungfish *Neoceratodus forsteri* (Krefft). *Comp. Biochem. Physiol., A: Comp. Physiol.* **152**, 162-167.

Reeves, R. B. (1980). A rapid micro method for obtaining oxygen equilibrium curves on whole blood. *Resp. Physiol.* **42**, 299-315.

Riebesell, U., Fabry, V. J., Hansson, L. and Gattuso, J.-P. (2010). Guide to best practices for ocean acidification research and data reporting: Publications Office of the European Union Luxembourg.

Ritz, C. and Streibig, J. C. (2005). Bioassay analysis using R. *J. Stat. Softw.* **12**, 1-22.

Safavi, A. and Bagheri, M. (2003). Novel optical pH sensor for high and low pH values. *Sensor Actuat. B-Chem.* **90**, 143-150.

Scott, G. R. (2011). Elevated performance: the unique physiology of birds that fly at high altitudes. *J. Exp. Biol.* **214**, 2455-2462.

Seibel, B., Chausson, F., Lallier, F., Zal, F. and Childress, J. (1999). Vampire blood: respiratory physiology of the vampire squid (Cephalopoda: Vampyromorpha) in relation to the oxygen minimum layer. *Exp Biol Online* **4**, 1-10.

Sick, H. and Gersonde, K. (1969). Method of continuous registration of oxygen binding curves of hemoproteins by means of a diffusion chamber. *Anal. Biochem.* **32**, 362–376.

Sick, H. and Gersonde, K. (1972). Theory and application of the diffusion technique for measurement and analysis of O2-binding properties of very autoxidizable hemoproteins. *Anal. Biochem.* **47**, 46-56.

Team, R. C. (2013). R: A Language and Environment for Statistical Computing. Vienna, Austria: R Foundation for Statistical Computing.

Truchot, J. P. (1976). Carbon dioxide combining properties of the blood of the shore crab, *Carcinus maenas* (L.): CO2-dissociation curves and Haldane effect. *J. Comp. Physiol.* **112**, 283-293.

van Holde, K. E., Miller, K. I. and Decker, H. (2001). Hemocyanins and Invertebrate Evolution. *J. Biol. Chem.* **276**, 15563-15566.

Weber, R. E., Behrens, J. W., Malte, H. and Fago, A. (2008). Thermodynamics of oxygenation-linked proton and lactate binding govern the temperature sensitivity of O-2 binding in crustacean (Carcinus maenas) hemocyanin. *J. Exp. Biol.* **211**, 1057-1062.

Weber, R. E., Campbell, K. L., Fago, A., Malte, H. and Jensen, F. B. (2010). ATP-induced temperature independence of hemoglobin-O2 affinity in heterothermic billfish. *J. Exp. Biol.* **213**, 1579-1585.

Wells, M. and Smith, P. (1987). The performance of the octopus circulatory system: a triumph of engineering over design. *Cell. Mol. Life Sci.* **43**, 487-499.

Wells, R. and Weber, R. (1989). The measurement of oxygen affinity in blood and haemoglobin solutions. *Techniques in comparative respiratory physiology: an experimental approach. Cambridge University Press, Cambridge*, 279-303.

Wirkner, C. S. and Richter, S. (2013). Circulatory system and respiration. *The natural history of the Crustacea* **1**, 376-412.

Zielinski, S., Sartoris, F. J. and Pörtner, H. O. (2001). Temperature effects on hemocyanin oxygen binding in an Antarctic cephalopod. *Biol. Bull. (Woods Hole)* **200**, 67-76.

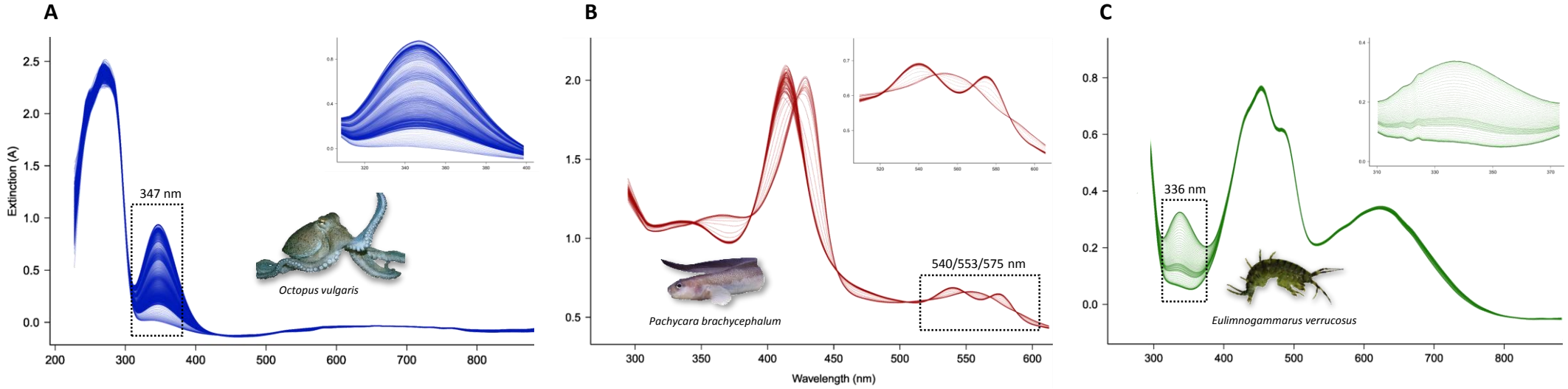
A
B
C
Extinction (A)
347 nm
Octopus vulgaris
Pachycara brachycephalum
540/553/575 nm
336 nm
Eulimnogammarus verrucosus
Wavelength (nm)

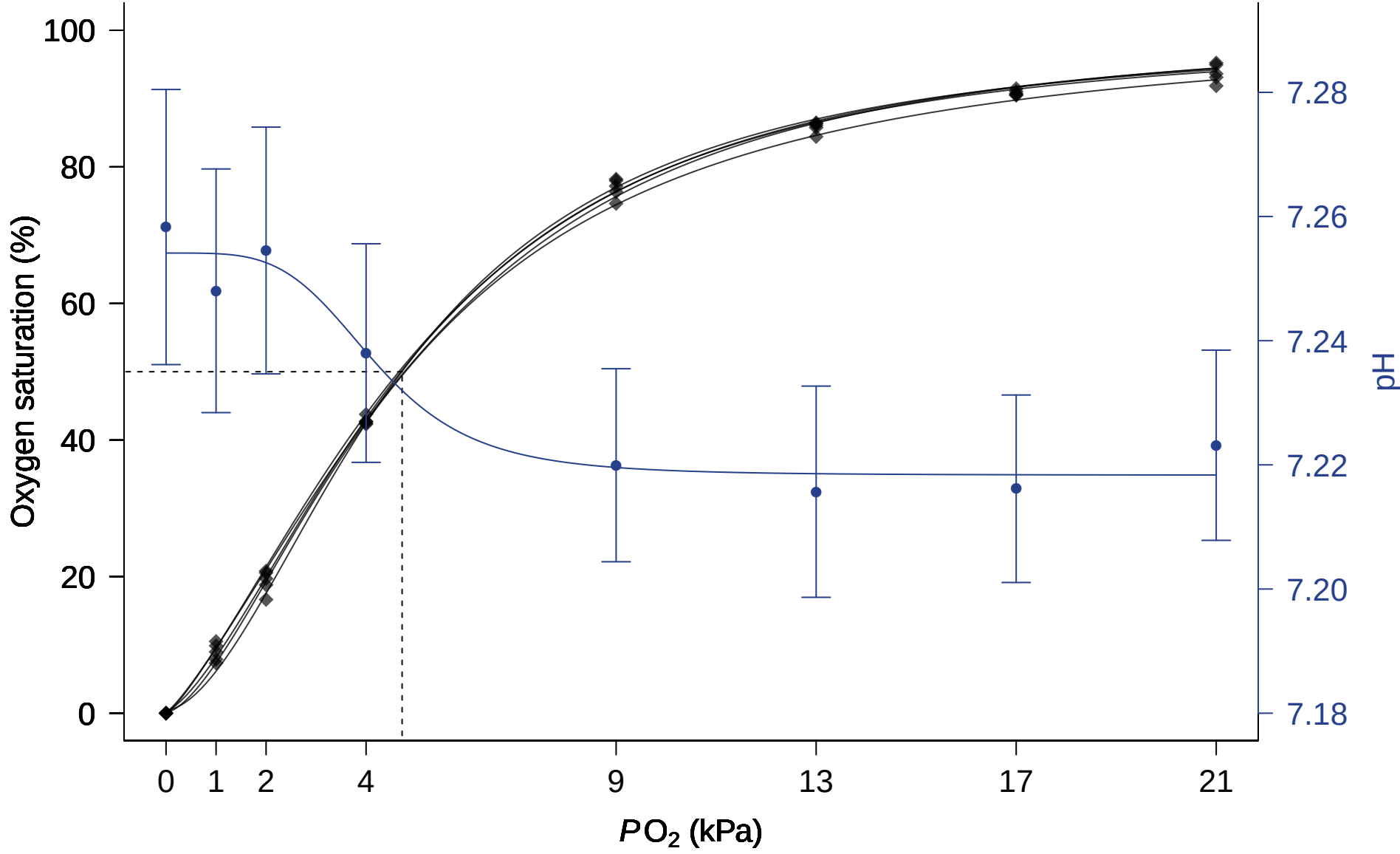
Oxygen saturation (%)
100
80
60
40
20
0
pH
7.28
7.26
7.24
7.22
7.20
7.18
0
1
2
4
9
13
17
21
PO2 (kPa)

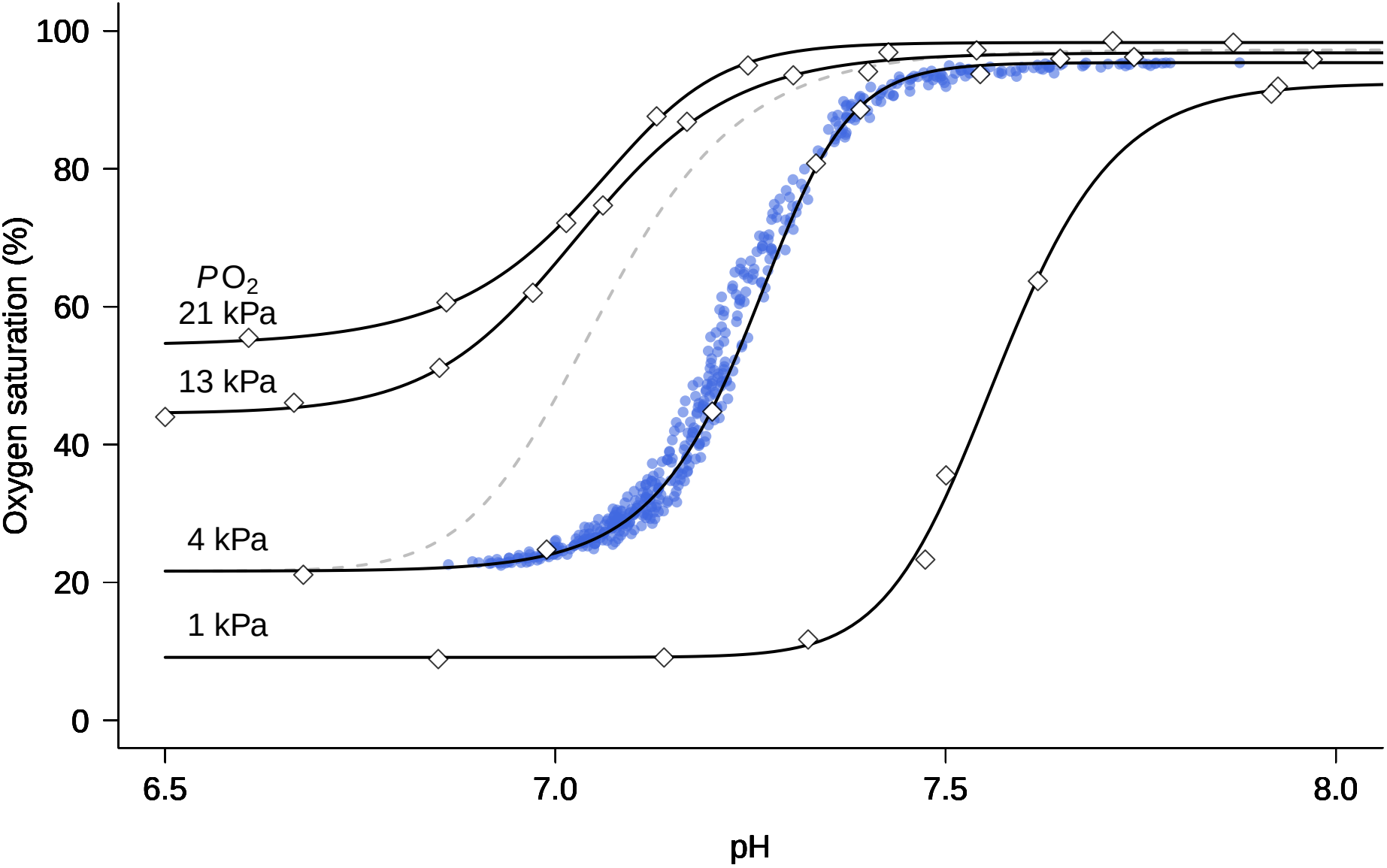
100
80
60
40
20
0
Oxygen saturation (%)
PO_2
21 kPa
13 kPa
4 kPa
1 kPa
6.5
7.0
7.5
8.0
pH

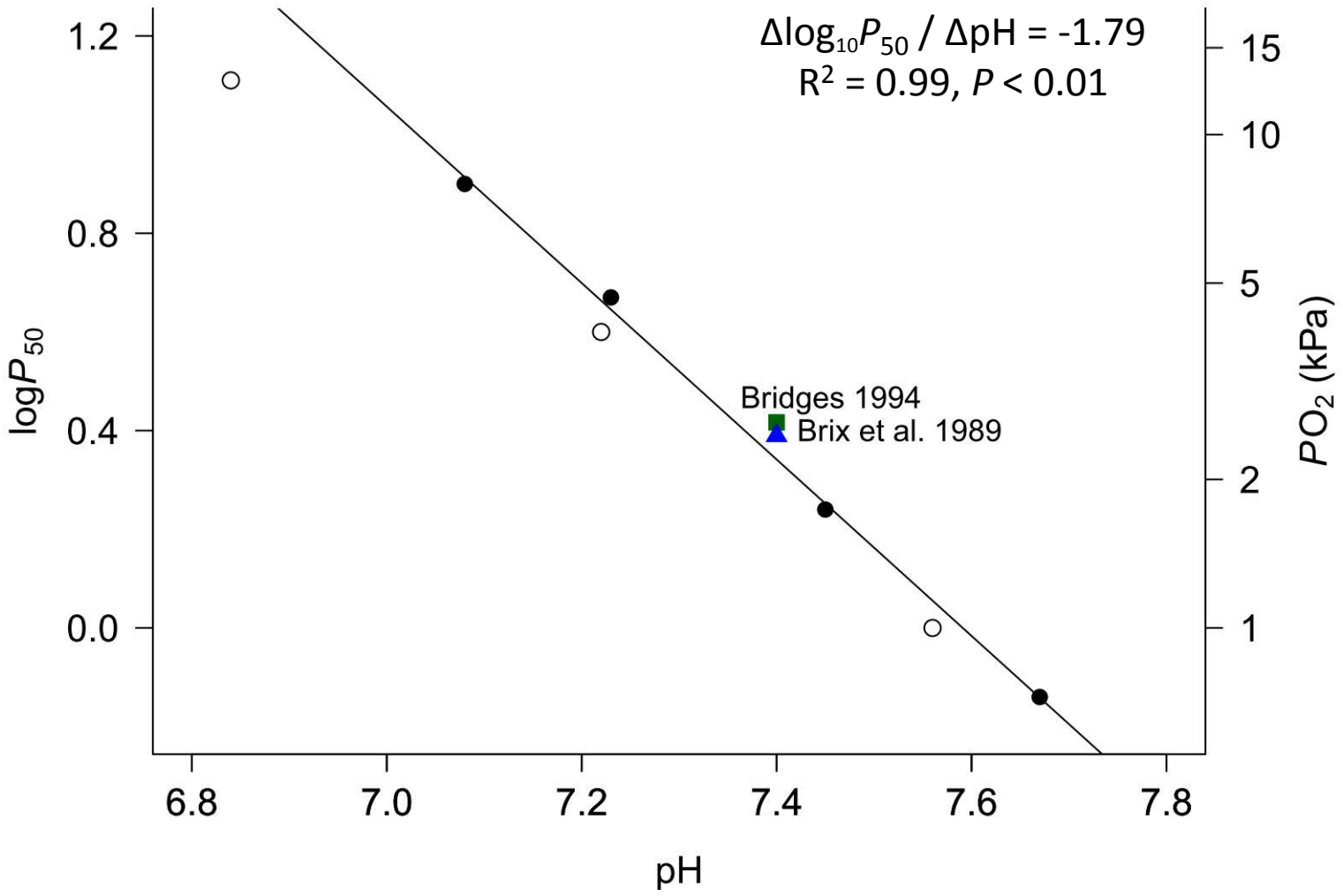
Δlog10P50 / ΔpH = -1.79
R2 = 0.99, P < 0.01
Bridges 1994
Brix et al. 1989
logP50
PO2 (kPa)
pH
1.2
0.8
0.4
0.0
15
10
5
2
1
6.8
7.0
7.2
7.4
7.6
7.8

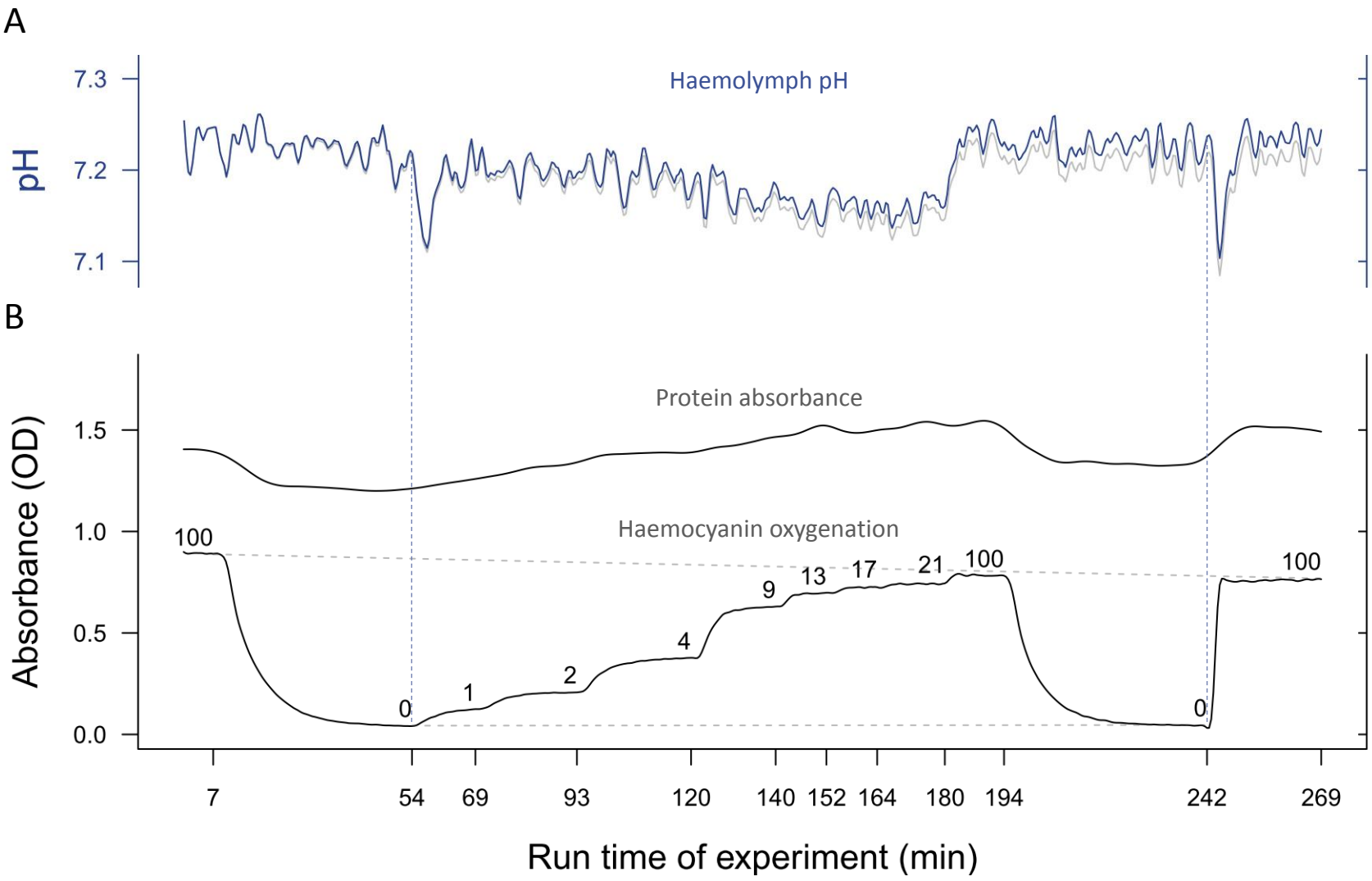
A
Haemolymph pH
pH
7.3
7.2
7.1
B
Protein absorbance
Haemocyanin oxygenation
Absorbance (OD)
1.5
1.0
0.5
0.0
100
0
1
2
4
9
13
17
21
100
0
100
7
54
69
93
120
140
152
164
180
194
242
269
Run time of experiment (min)

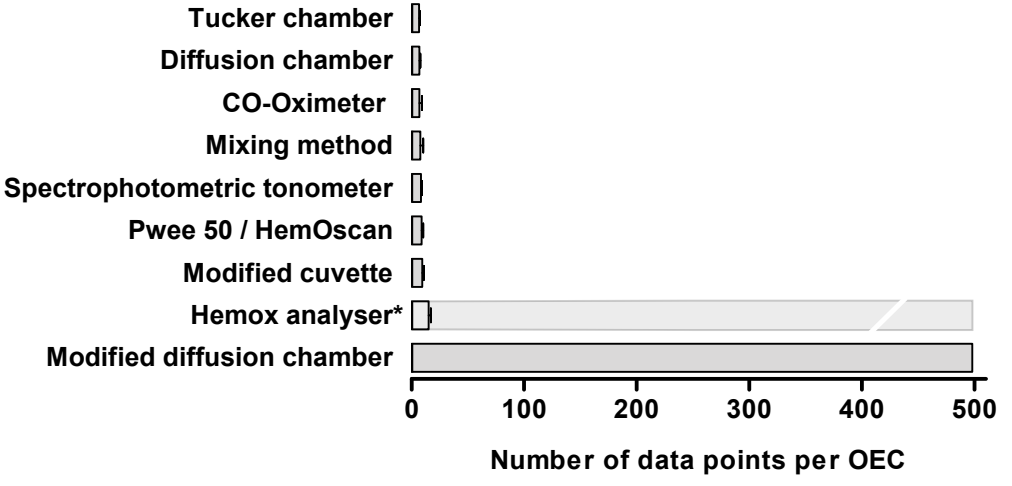

*While some studies record fewer data points, recording intervals may be maximised to 1/sec

A

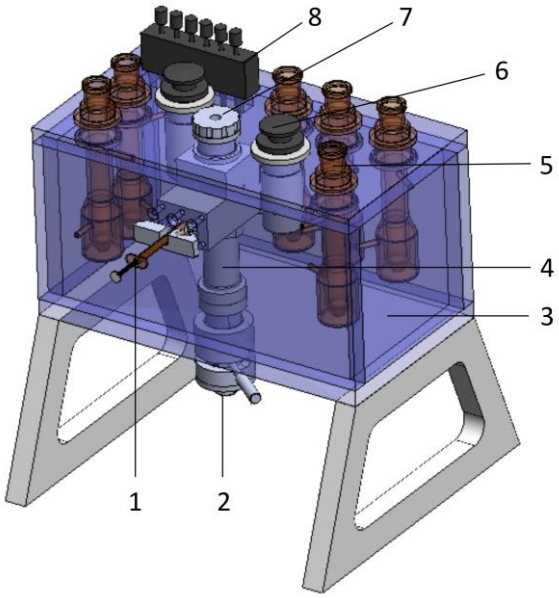

B

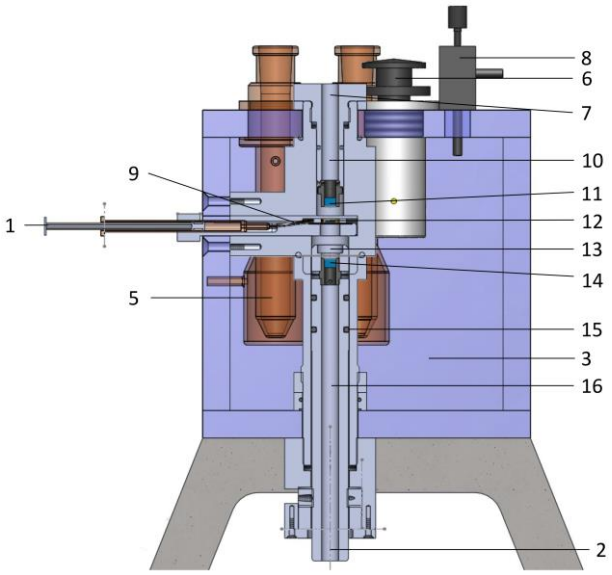

1. Syringe housing for the pH micro optode
2. Fibre optic cable exit to the spectrophotometer
3. Temperature controlled water reservoir
4. Central cylinder containing optical devices
5. Gas-washing flask
6. Control wheel for gas distribution
7. Fibre optic cable inlet from the light source
8. Control panel for gas inflow
9. Needle housing for the fibre optic sensor tip
10. Upper custom made tube, housing a collimating lens and the fibre optic cable from the light source
11. Upper collimating lens
12. Blood sample spread on a glass plate
13. Spacer to keep 10 mm minimal distance between collimating lens and sample
14. Lower collimating lens
15. Rubber to seal lower tubing
16. Lower custom made tube, housing a collimating lens and the fibre optic cable leading to the spectrophotometer

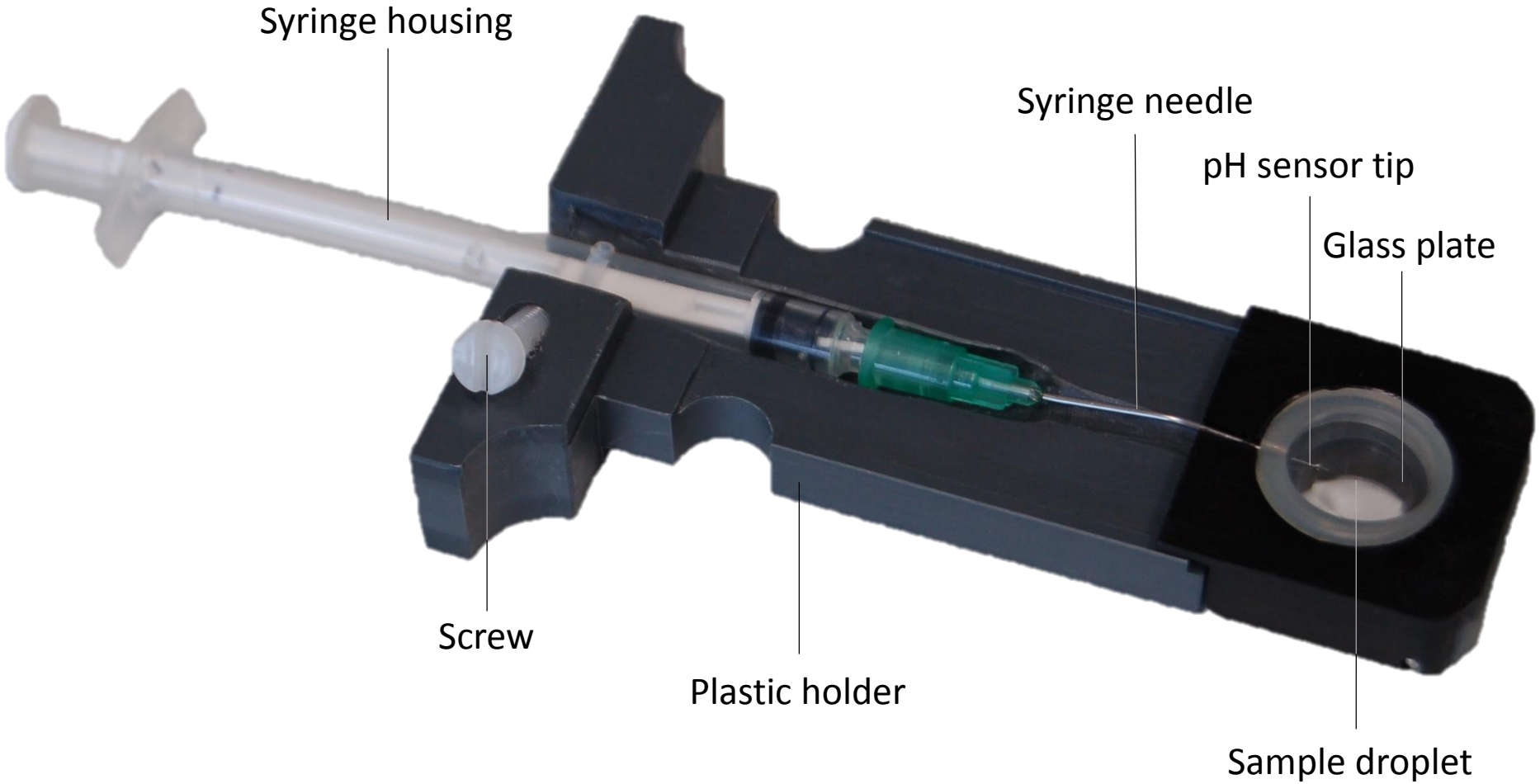
Syringe housing
Syringe needle
pH sensor tip
Glass plate
Screw
Plastic holder
Sample droplet